CAL-2789

National Aeronautics and Space Administration

ASCA

FINAL TECHNICAL REPORT

FOR NASA GRANT NAG 5-3307

Submitted to:

Dr. Nicholas White, Code 668
Lab for High Energy Astrophysics
NASA/Goddard Space Flight Center
Greenbelt, MD 20771

Submitted by:

The Trustees of Columbia University
in the City of New York
351 Engineering Terrace
New York, New York 10027

Prepared by:

Columbia Astrophysics Laboratory
Departments of Astronomy and Physics
Columbia University
550 West 120^{th} Street
New York, New York 10027

Titles of Research:

"Monitoring MRK 509: The Origin of the Reprocessor" and "Broad Band X-Ray Spectrum of Narrow Line Seyfert 1 AKN 564"

Principal Investigators:

Jules P. Halpern & Karen M. Leighly

Period Covered by Report:

1 August 1996 – 31 January 1998

March 1998

Final Report for NASA Grant NAG 5-3307, (ASCA)

Monitoring Mrk 509: The Origin of the Reprocessor Broad-band X-ray Spectrum of Narrow Line Seyfert 1 Akn 564

K. M. Leighly, J. P. Halpern et al.

March 23 1998

Mrk 509: The ten monitoring observations of Mrk 509 were made successfully between October 20 and November 26 last year. These observations were simultaneous with *RXTE* observations. A preliminary analysis of the *RXTE* observations has been done, and the light curve is shown in Figure 1. Our aim in this experiment is to determine the location of the emission region of the reflection component by reverberation mapping. This component could be emitted from the accretion disk, within 100 Schwartzschild radii (R_s) from the source. Note that the monitoring interval of 2.5 days corresponds to $100R_s$ for a 2×10^8 solar mass black hole, which may be appropriate for this luminous object. In that case, we would expect the reflected component to vary along with the direct flux, and there should be no spectral variability between observations. Alternatively, the reflected emission could come from the molecular torus, several parsecs from the nucleus. In that case, the reflection component flux should not vary. The light curve in Figure 1 shows that during the monitoring period, the target varied in an ideal way, since significant variability was observed between observations and yet the most rapid variability is apparently sampled.

The analysis of this data is not yet completed. The measurement of the reflection component in the combined *ASCA* and *RXTE* spectra depends critically on the *RXTE* background subtraction and calibration, but these have not yet progressed to the point where the analysis can be done.

Akn 564: The *ASCA* observation of the narrow-line Seyfert 1 (NLS1) galaxy was performed December 24 1996. Preliminary analysis indicates it was quite bright during the observation at 1.8 counts/s in the SIS. The source was very variable during the observation. While the total amplitude of variability was not so high, significant rapid variability occurred during nearly every orbit. Analysis indicates that the spectrum is rather similar to that of PG 1244+026 in that there an excess in flux near 1 keV which can be fit by an emission line model with equivalent width of ~ 60 eV. The origin of this peculiar feature is unknown and is under further investigation. However, we speculate that the line may originate in an ionized accretion disk. A similar scenario was postulated for the NLS1 PG 1244+026 (Fiore et al. 1998).

The spectral and variability results from the *ASCA* observation will be presented as a part of the sample of *ASCA* observations of NLS1s described below (Leighly et al. 1998 in preparation). These data will also be combined with a simultaneous *RXTE* observation and written up separately (Edelson et al. 1998 in preparation).

Archival ASCA Observations of NLS1s: We are in the process of performing a comprehensive and uniform analysis of 24 *ASCA* observations of 22 Narrow-line Seyfert 1 galaxies. Preliminary results were discussed in an invited talk at the 23rd IAU General Assembly "Joint Discussion on High Energy Transients" and in a contributed talk at the "Accretion Processes in Astrophysical Systems: Some Like it Hot". The results are described

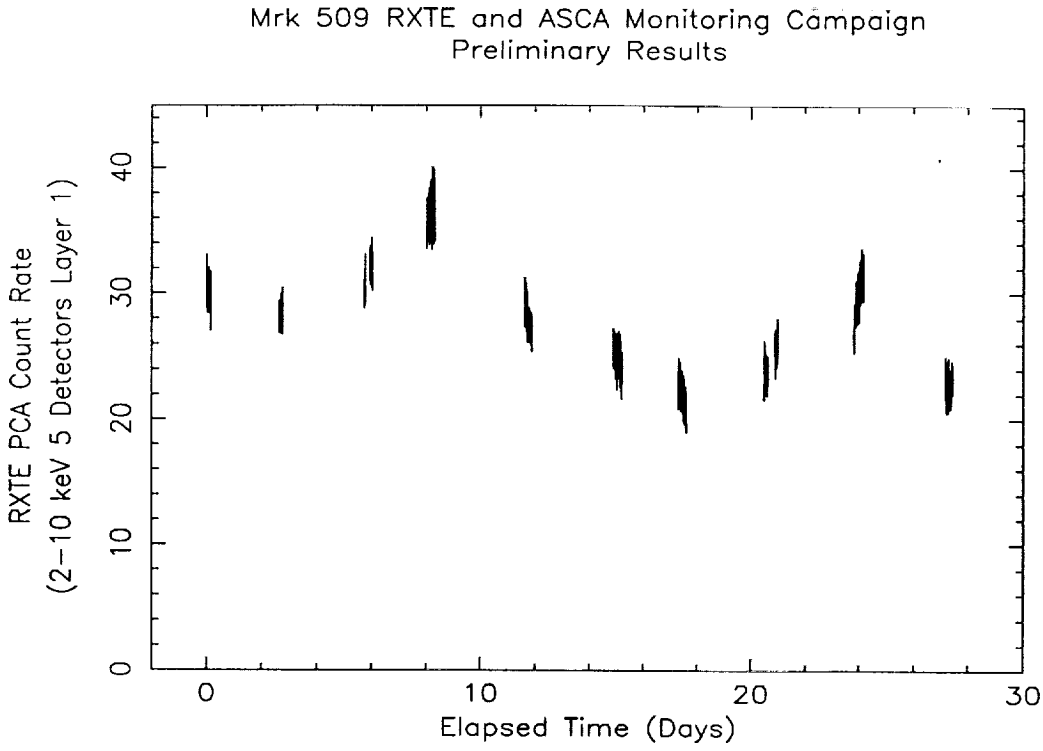

Figure 1: *RXTE* lightcurve from Mrk 509 simultaneous *ASCA* and *RXTE* monitoring campaign.

in the accompanying proceedings papers (Leighly 1998a; Leighly 1998b). This work was also presented as a contributed talk at the High Energy Astrophysics Division meeting in Estes Park, Colorado (abstract only).

During this analysis, we found a peculiar absorption feature near 1 keV in the spectra of three NLS1s, and performed a detailed spectral analysis of the data from these three objects. This feature suggests the presence of partially ionized material in the line of sight, but the derived edge energy near 1 keV is too high if the absorber is in the galaxy rest frame. However, the absorbing material could be in the process of being ejected from the nucleus at relativistic velocities, resulting in blueshifted oxygen absorption lines or edges. This explanation is appealing when we note the remarkable similarities between NLS1s and broad absorption line quasars, which are well known for the broad absorption lines in their UV spectra indicating outflowing material with velocities up to about 10% of the speed of light. For example, many NLS1s and BALQSOs show strong or extreme Fe II emission and weak [O III] emission. While these emission lines are generally anticorrelated, objects which have the strongest Fe II emission and weakest or no [O III] emission tend to be either low ionization BALQSOs or NLS1s. Many NLS1s and BALQSOs have red optical continuum spectra, and relatively strong infrared emission. In fact, infrared selection seems to pick out a substantial number of low ionization BALQSOs and NLS1s. Finally, both classes are predominantly radio quiet. This paper was published last year in the accompanying paper

(Leighly et al. 1997a) and it also appeared in a proceedings (Leighly, Mushotzky & Nandra 1997). It was also presented as a contributed talk at the ASCA Cherry Blossom Workshop (April 1–4 1997, Washington D.C.) and the paper was also presented as a poster at the American Astronomical Society meeting in Washington, DC in January 1998.

We also found a warm absorber in the *ASCA* spectrum of one of the NLS1s, IRAS 17020+4544. Since it has a reddened optical spectrum, it seemed possible that the ionized absorption in this object could be coincident with dust. Dust causes reddening in the optical spectrum, but it can also cause polarization. Imaging polarimetry and spectropolarimetry of IRAS 17020+4544 were subsequently obtained at McDonald and Lick Observatories and the high polarization was confirmed. To investigate whether ionized absorption in the X-ray spectrum is generally associated with the presence of polarization in the optical spectrum, results from a sample of Seyfert 1 and 1.5 galaxies were compiled. All of the highly polarized Seyferts had warm absorbers in their X-ray spectra. Spectropolarimetry provides information about the geometry of the emission and scattering regions, and the coincidence of dust and the warm absorber constrains the conditions and location of this material. Therefore, this result holds deep implications for the origin, location and physical composition of the scattering, absorbing and emitting material in Seyfert 1 galaxies. This result was published last year in the accompanying paper (Leighly et al. 1997b). It was presented as a poster paper at the High Energy Astrophysics Divisional meeting in November 1997 in Estes Park, Colorado, and also at the "Structure and Kinematics of Quasar Broad Line Regions" in Lincoln, Nebraska in March 1998.

Bibiography

X-ray Variability in Active Galactic Nuclei
K. M. Leighly, proceedings of the IAU "Joint Discussion on High Energy Transients", Kyoto, Japan, August 26–27 1997 in press

A Comprehensive Spectral and Variability Study of Narrow-Line Seyfert 1 Galaxies Observed by ASCA
K. M. Leighly, Proceedings of "Accretion Processes in Astrophysical Systems: Some Like it Hot", College Park, Maryland, October 13–15, 1997, in press

Evidence for Relativistic Outflows in Narrow-line Seyfert 1 Galaxies
K. M. Leighly, R. F. Mushotzky, K. Nandra, & K. Forster, 1997, ApJL, 489, L25

Evidence for Relativistic Outflows in Narrow-line Seyfert 1 Galaxies
K. M. Leighly, R. F. Mushotzky, & K. Nandra, 1997, Proceedings of *Mass Ejection from AGN*, ed. N. Arav, I. Shlosman, & R. J. Weymann (ASP: San Francisco) p. 155

Evidence for Relativistic Outflows in Narrow-line Seyfert 1 Galaxies
K. M. Leighly, R. F. Mushotzky, & K. Nandra, 1997, Bull. American Astron. Soc. 191, #104.13 (abstract only)

The Optical Polarization and Warm Absorber in IRAS 17020+4544
K. M. Leighly, L. E. Kay, B. J. Wills, D. Wills, & D. Grupe 1997, ApJL, 489, L137

Karen M. Leighly
Associate Research Scientist
Columbia Astrophysics Laboratory
Columbia University

X-RAY VARIABILITY IN ACTIVE GALACTIC NUCLEI

Two Things That Everybody Should Know

KAREN M. LEIGHLY
Columbia Astrophysics Laboratory, Columbia University
538 West 120th Street, New York, NY 10027
leighly@ulisse.phys.columbia.edu

Proc. IAU
Joint Discussion on
High Energy Transients
Kyoto, Japan
August 26, 27 1997

1. Introduction

X-ray variability is a distinguishing property of Active Galactic Nuclei (AGN), and the energetics and time scales of the emission dictate that the X-rays must originate very close to the central engine. In this review I discuss two basic topics from AGN variability research. The first is the correlation of the variability time scale with the X-ray luminosity, and the second is the structure of the X-ray light curve. In each case, I first review the old results that have been known for approximately the last 10 years and then I discuss very new results which may force us to modify our ideas about the origin of AGN X-ray variability. Note that I am discussing the variability of non-blazar type AGN.

2. AGN Variability Time Scales

2.1. THE OLD RESULTS

No matter how you measure it, the time scale of X-ray variability is always observed to be inversely correlated with the 2–10 keV luminosity. Lower luminosity Seyfert galaxies vary on very short times scales, sometimes shorter than 1000 seconds, while higher luminosity AGN vary significantly only on much longer time scales of days. This result was first reported by Barr & Mushotzky (1986) who estimated the doubling time scale by extrapolating observed variability, but the correlation is also found when the time scale is measured in other, more robust ways. Lawrence & Papadakis (1993) found that the amplitude of the variability power spectrum (PDS) at a particular frequency is inversely proportional to the luminosity. This parameter is related to the variability time scale if all AGN have the same shape PDS, as was found in their sample. More recently, from a sample of *ASCA* observations of Seyfert galaxies, Nandra et al. (1997) found that the excess variance, defined as the measured variance of the light curve minus the variance due to measurement error, is inversely proportional to the 2–10 keV luminosity. Since the slope of the PDS is steep down to at least 1×10^{-3} Hz (see Section 3.1), the measured excess variance will be larger for longer observations. However, this parameter can be used for *ASCA* light curves since all the observations are about the same length and have approximately the same sampling pattern.

What could be the physical origin of this correlation? The time scale of variability can be related to the source size, since the emission region must be smaller than the time scale times the speed of light. Then the Schwartzschild radius relates the source size to the black hole mass. If accretion onto a black hole powers AGN and if the emission is isotropic, the luminosity must be smaller than the Eddington value, also related to the black hole mass. Therefore, if the luminosity is the same fraction of the Eddington value in all objects, it is natural for more luminous objects to vary more slowly. However, the dependence does not appear to be exactly one-to-one, possibly a result of a shallow increase in Eddington fraction in more luminous objects; see Lawrence & Papadakis 1993 and Nandra et al. 1997 for further discussion.

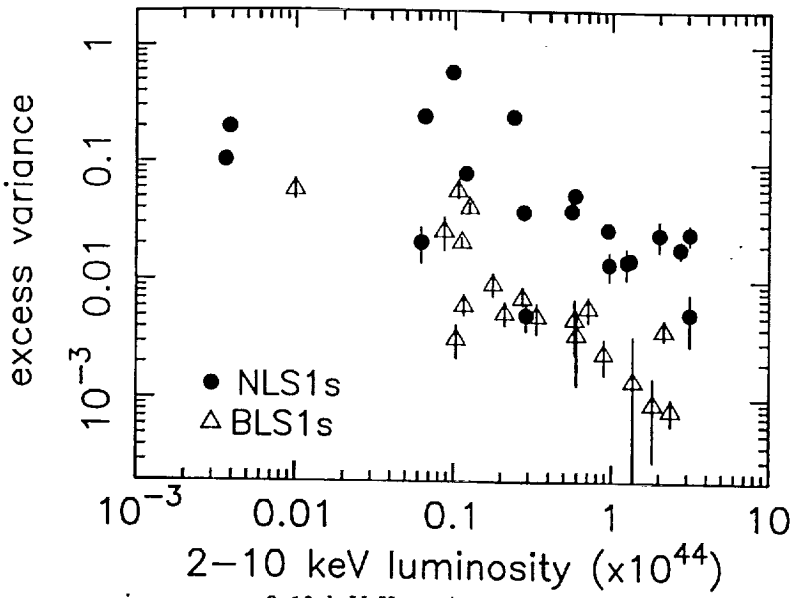

Figure 1. The excess variance versus 2–10 keV X-ray luminosity from *ASCA* observations of AGN. The open triangles, from Nandra et al. 1997, mark AGN with broad optical lines and trace the established correlation of variability time scale with luminosity. The solid circles mark the narrow-line Seyfert 1s (Leighly et al. 1997b). There also seems to be a rough inverse correlation with luminosity but for a given luminosity the excess variance from the NLS1s is generally significantly larger than that from AGN with broad optical lines.

2.2. THE NEW RESULTS

New observations show that things do not appear to be as simple as we thought when you consider, surprisingly enough, the optical classification of the AGN. Narrow-line Seyfert 1 galaxies (NLS1s; not to be confused with NELGs, NLXGs, or Seyfert 2s) are identified by their narrow permitted lines which are only slightly broader than the forbidden lines (Hβ FWHM < 2000 km/s), low [O III]λ5007 to Hβ ratio, and typically strong Fe II emission (Osterbrock & Pogge 1985; Goodrich 1989). Observations using *ROSAT* revealed the first evidence that this class of AGN often exhibits high amplitude, rapid variability (e.g. Boller, Brandt & Fink 1996; Forster & Halpern 1996). Figure 1 shows the excess variance from *ASCA* observations of NLS1s overlaid on the results found by Nandra et al. for Seyferts with broader optical lines (Leighly et al. 1997b). There appears to be again a rough correlation between excess variance and luminosity; however, for a given luminosity, the NLS1 excess variance is typically an order of magnitude higher.

What could be the origin of this result? One possibility is that NLS1s are characterized by a relatively higher accretion rate. If a higher accretion rate relative to the Eddington value implies a higher luminosity, then for a particular X-ray luminosity the black hole mass can be smaller in NLS1s implying more rapid variability. This scenario is supported by the fact that the X-ray spectrum of NLS1s is also different from that of Seyfert 1s with broader optical lines. Characterized by a stronger and hotter soft X-ray excess component, and a steeper power law (Pounds, Done & Osborne 1995; Brandt, Mathur & Elvis 1997), this is reminiscent of the spectrum of high state Galactic black hole candidates, which are also believed to be accreting at a higher fraction of the Eddington rate.

3. The Structure of the X-ray Light curve

3.1. THE OLD RESULTS

The *EXOSAT* satellite (1983–1986) had a highly eccentric orbit which allowed it to continuously observe a target for up to three days. In contrast, more recent X-ray missions including *Ginga* and *ASCA* have nearly circular orbits and therefore observations are interrupted every ~ 96 minutes by earth occultation and regions of high particle background. Toward the end of the mission, *EXOSAT* made long observations of a handful of rapidly variable AGN. It is from these data that we have gained most of our knowledge about the structure of the X-ray light curve, due to the great difficulty

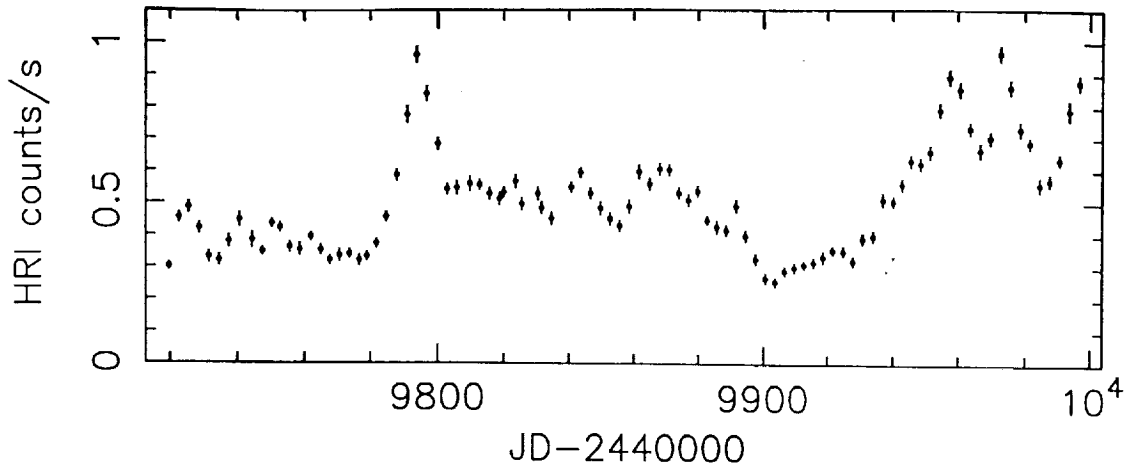

Figure 2. The soft X-ray light curve from the 1995 monitoring of the broad-line radio galaxy 3C 390.3 using the *ROSAT* HRI (Leighly et al. 1997a). The flares and quiescent periods before and after the flares are characteristic of nonlinear variability (Leighly & O'Brien 1997).

of doing time series analysis on light curves with gaps. The result is that the light curves can be described by a steep and essentially featureless power law with $P(\nu) \propto \nu^{-\alpha}$ where the slope $\alpha \approx 1.5$ between 10^{-5} and 10^{-3} Hz (Lawrence et al. 1987; McHardy & Czerny 1987; McHardy 1989; Green, McHardy & Lehto 1993; Lawrence & Papadakis 1993). Because the power law is featureless, the slope of the power law is the only information available to constrain physical models.

What kinds of model can explain this result? Shot noise, composed of randomly occurring, exponentially decaying flares, cannot directly explain this result since $\alpha = -2$ is predicted. However, if there is a range of decay time scales a flatter slope would be found over a limited frequency range (Lehto 1989). The rotating hot spot model attempts to explain the variability in a more physical way. The emission from active regions distributed on a Keplerian accretion disk will be modulated by Doppler and gravitational effects and occultations, and the superimposed individual light curves will produce a steep power-law PDS (e.g. Abramowicz et al. 1991; Abramowicz et al. 1992; Zhang & Bao 1991; Bao & Østergaard 1995). AGN broad band continuum spectra support this model. Hard X-rays are thought to be produced in a corona lying above a disk, the source of the optical and UV emission. Since the UV luminosity L_{UV} is typically much larger than L_X the corona should not cover the disk completely but rather be patchy (Haardt, Maraschi & Ghisellini 1994).

3.2. NEW RESULTS

In 1995 we observed the broad-line radio galaxy 3C 390.3 every three days for nine months, obtaining the first well-sampled AGN X-ray light curve on these time scales (Leighly et al. 1997a; Figure 2). Considerable structure is seen, including flares and periods of quiescence before and after the flares where the variability is significantly reduced. This structure is characteristic of *nonlinear* variability (e.g. Vio et al. 1992). Here "nonlinear" is used in the mathematical sense and it means that the light curve can not be modeled as a sum of *independent* events. Time series analysis found that nonlinearity was detected with $> 6\sigma$ confidence (Leighly & O'Brien 1997). This result is important because it rules out shot noise and rotating hot spot models discussed in the previous section since in those models the events which superimpose to form the power-law PDS are independent.

The flares and reduction in variability before and after the flares is similar to that observed in *Ginga* light curves from the Galactic black hole candidate Cygus X-1 (Negoro et al. 1995). A self-organized critical (SOC) disk model was developed to explain this result (Mineshige, Ouchi & Nishimori 1994). The disk is assumed to be composed of numerous reservoirs, and when a critical density is reached in a reservoir, an instability is triggered, and an avalance of accretion results in a flare. The reservoirs are *coupled* providing the essential nonlinearity in this model. Large flares result when the instability is triggered in many adjacent reservoirs. A reduction in variability is produced after large flares because the reservoirs must fill again, while it is found before the large

flares because they are more likely to occur if no small flares have happened to release the potential energy. This model cannot be directly applied to AGN, since the X-rays most likely do not originate in the disk; however, SOC models are quite general.

Nonlinear variability has been recently reported in a series of *ROSAT* monitoring observations of NLS1 IRAS 13224−3809 (Boller et al. 1997) and in fact it is also detectable in the *ASCA* light curve from this object (Leighly et al. 1997b). However, it was not detected in the set of *EXOSAT* long observations discussed in the previous section, although several groups have looked (Krolik, Done & Madejski 1993; Lehto, Czerny & McHardy 1993; Czerny & Lehto 1997). Low signal-to-noise is a possible problem. The SNR of the 3C 390.3 light curve is about 30, and if I degrade the data by adding and subtracting noise, I lose the nonlinearity detection at SNR $\approx$ 10. An alternative exciting possibility is that some objects exhibit linear while others exhibit nonlinear variability, and detection of nonlinearity could prove to be an important physical diagnostic.

4. Future Prospects

The field of AGN X-ray variability study is in a somewhat primitive state, especially compared to the study of variability of Galactic objects. The problem is that AGN generally have much lower fluxes than Galactic objects, and therefore low signal to noise can be a problem. A second problem is that AGN have much longer variability time scales and therefore the variability cannot be not adequately sampled in typical one-day observations. Finally, the gaps in the light curves from low earth orbit satellites are a severe impediment for detailed time series analysis. However, current and new missions soon to be launched should revolutionize the field. *AXAF* and *XMM* will have highly eccentric orbits like *EXOSAT* but much more sensitive detectors. Light curves from long observations of rapidly variable AGN will be amazing. *RXTE*, which has the advantage that about 1/2 of the sky is available during the entire year, is currently monitoring a handful of AGN with intervals of days over long periods of time. The results of these observations also should be very exciting. *ROSAT* is still being used to monitor soft AGN such as NLS1s. Finally, the next generation of all-sky monitors, including the proposed *Lobster* mission and *MAXI* which will be placed on the Japanese module of the space station, should be sensitive enough to obtain SNR=5 detections of 1000 AGN per day, and high SNR flux measurements of about 25.

References

Abramowicz, M., Bao, G., Lanza, A, & Zhang, X.-H. 1991, A&A, 245, 454
Abramowicz, M. A., Lanza, A., Spiegel, E. A., & Szuszkiewicz, E. 1992, Nature, 356, 41
Bao, G., & Ostergaard, E., 1995, ApJ, 443, 54
Barr, P., & Mushotzky, R. F. 1986, Nature, 320, 421
Boller, T., Brandt, W. N., Fabian, A. C., & Fink, H. H., 1997, MNRAS, 289, 393
Boller, Th., Brandt, W. N. & Fink, H., 1996, A&A, 305, 53
Brandt, W. N., Mathur, S., & Elvis, M., 1997, MNRAS, 285, 25
Czerny, B., & Lehto, H. J., 1997, MNRAS, 285, 365
Forster, K. & Halpern, J. P. 1996, ApJ, 468, 565
Goodrich, R. W., 1989, ApJ, 342, 224
Green, A. R., McHardy, I. M., & Lehto, H. J., 1993, MNRAS, 265, 664
Haardt, F., Maraschi, L., & Ghisellini, G. 1994, ApJL, 432, 95
Krolik, J., Done, C., & Madejski, G., 1993, ApJ, 402, 432
Lawrence, A., et al. 1987, Nature, 325, 694
Lawrence, A., & Papadakis, I. E., 1993, ApJL, 414, 85
Lehto, H. J., Czerny, B., & McHardy, I. M., 1993, MNRAS, 261, 125
Leighly, K. M., & O'Brien, P. T., 1997, ApJL, 481, 15
Leighly, K. M., et al. 1997a, ApJ, 483, 767
Leighly, K. M., et al. 1997b, in preparation
Lehto, H. 1989. *Proc. 23rd ESLAB Symp.*, eds. J. Hunt and B. Battrick (Paris: ESA) p. 499
McHardy, I. M. 1989. *Proc. 23rd ESLAB Symp.*, eds. J. Hunt and B. Battrick (Paris: ESA) p. 1111
McHardy, I., & Czerny, B., 1987, Nature, 325, 696
Mineshige, S., Ouchi, B. & Nishimori, H. 1994, PASJ, 46, 97
Nandra, K., et al. 1997, ApJ, 476, 70
Negoro, H., Kitamoto, S., Takekuchi, M., & Mineshige, S. 1995, ApJL, 452, 49
Osterbrock, D. E. & Pogge, R. W. 1985, ApJ, 297, 166
Pounds, K. A., Done, C., & Osborne, J. P., 1995, MNRAS, 277, 5P
Vio, R., et al. 1992, ApJ, 391, 518
Zhang, X.-H., & Bao, G., 1991, A&A, 246, 21

Proc. "Accretion Processes in Astrophysical Systems: Some like it Hot"
Oct 13-15 1997

A Comprehensive Spectral and Variability Study of Narrow-Line Seyfert 1 Galaxies Observed by ASCA

Karen M. Leighly

Columbia Astrophysics Laboratory, Columbia University, New York, NY 10027
leighly@ulisse.phys.columbia.edu

Abstract. I report the results of a comprehensive analysis of a sample 23 *ASCA* observations of 21 narrow-line Seyfert 1 galaxies (NLS1s). In comparison with Seyfert 1 galaxies with broader optical lines, NLS1s are more variable as parameterized by the excess variance during a typical 1 day observation. There is a strong correlation between excess variance and luminosity, and also a tendency for objects with steeper overall *ASCA* spectra to show higher excess variance. Eleven objects had very steep hard X-ray photon indices. A soft excess component was required in 15 spectra, and significant absorption was found in 6 objects. Three NLS1s showed features near 1 keV which have been interpreted as signatures of absorption in relativistically outflowing gas. Three others have an emission feature near 1 keV which was interpreted as emission from photoionized neon or iron in PG 1244+026.

INTRODUCTION

Narrow-line Seyfert 1 galaxies (NLS1s) are distinguished by their optical line properties. They have narrow permitted lines, with FWHM Hβ $<$ 2000 km/s; the forbidden lines are relatively weak, with [O III]/Hβ $<$ 3; they often show strong Fe II emission [1,2]. *ROSAT* observations demonstrated that they also have distinctive X-ray properties. They have steep soft X-ray spectra and they often show rapid variability [3–5]. However, the X-ray spectral and variability properties of NLS1s cannot be studied adequately using *ROSAT* data because of the poor spectral resolution and limited band pass of the PSPC, and because the observations were generally not contiguous. *ASCA* observations provide much more information because of the broad band pass and the typically longer than one day observations. I present results from analysis of a sample of 23 *ASCA* observations of 21 narrow-line Seyfert 1 galaxies.

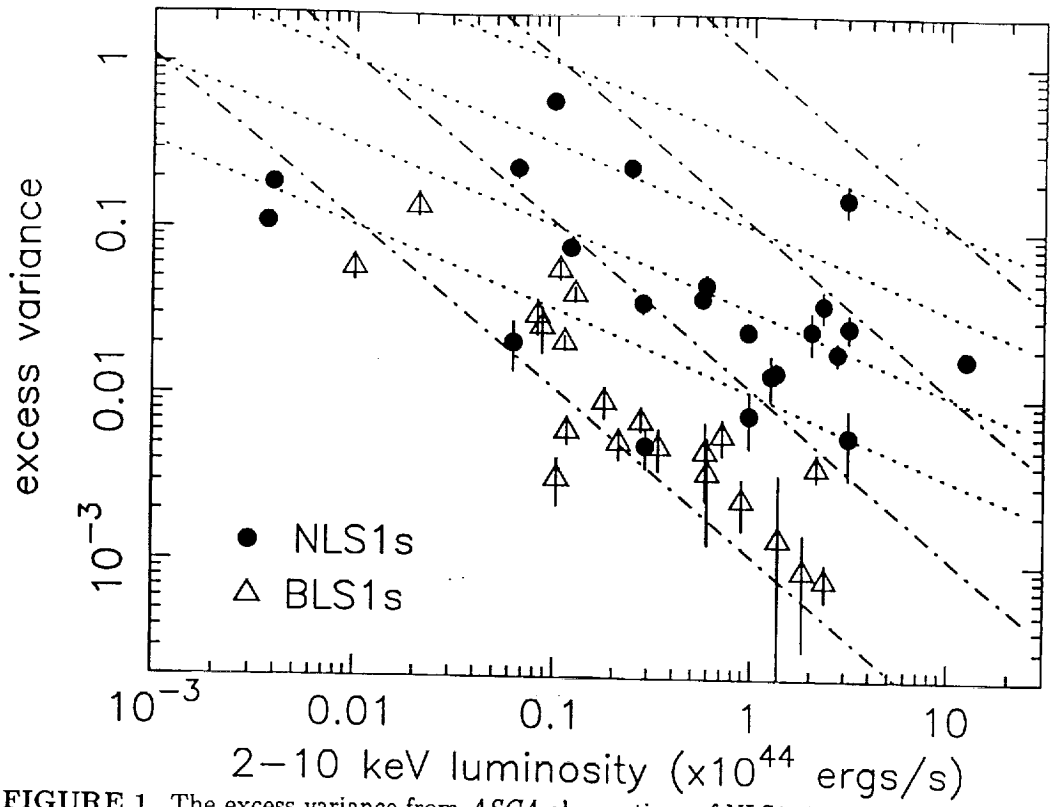

FIGURE 1. The excess variance from *ASCA* observations of NLS1s is consistently higher than that from Seyfert 1s with broader optical lines at a particular 2–10 keV luminosity. Superimposed are lines of either constant efficiency or constant mass accretion rate, where the lines are separated by a decade of that parameter. Dotted and dot-dashed lines correspond to assumed variability power spectra proportional to $1/f^{1.5}$ and $1/f^2$ respectively.

VARIABILITY RESULTS

Significant variability was observed from all objects except Mrk 507 and Kaz 163. The excess variance, defined as the true variance minus the variance due to measurement error, provides an estimate of the inverse of the variability time scale, assuming that for all objects the sampling pattern is the same and the variability power spectrum has the same slope [6]. The excess variance versus hard X-ray luminosity is shown for a sample of Seyferts in Figure 1. This figure also shows the lines of either constant accretion rate or constant efficiency of conversion of accretion potential energy to radiation. For a given luminosity, NLS1s show a consistently higher excess variance than Seyfert 1s with broader optical lines. This can be most simply interpreted as evidence that NLS1s are characterized by either a higher accretion rate or efficiency or both.

The excess variability also seems to be related to the shape of the X-ray spectrum among the NLS1s. I define an X-ray slope (α_{xx}) to be the energy index between the unabsorbed fluxes at 0.7 keV and 4 keV, the approximate logarithmic mean

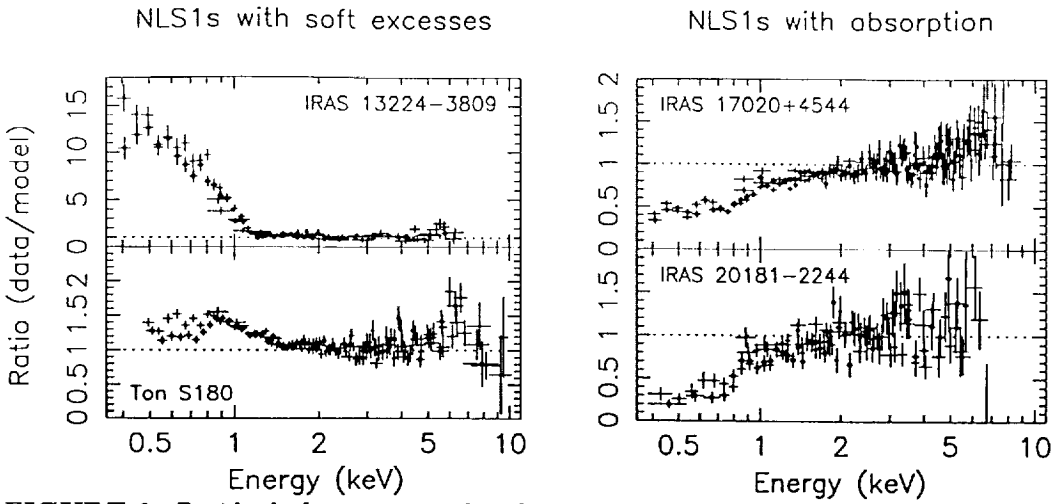

FIGURE 2. Residuals from a power law fit in the 2–5 keV and > 8.0 keV bands. Small and large circles show SIS0 and SIS1 respectively. LEFT: There are a range of sizes of the soft excess. In IRAS 13324-3809 this component is very strong, while in Ton S180 it is weaker and apparently continues to a higher energy. The discrepancy between SIS0 and SIS1 is probably due to RDD effects. RIGHT: The absorbing material in IRAS 17020+4544 is clearly ionized [7] and there is marginal evidence that it may be also in IRAS 20181-2244 [8].

energies of the soft and hard spectral components, respectively. There is a rough correlation between the excess variance and α_{xx}. However, note that this does not account for the correlation between luminosity and excess variance.

SPECTRAL RESULTS

The average spectra from each observation were fitted with a variety of models, and the results are summarized as follows:

- It has been reported that the hard X-ray photon index of NLS1s is generally steeper than that of Seyferts with broader optical lines [3]. In this sample, the hard X-ray photon index of the NLS1s is often very steep but not always. Eleven objects have photon indices near 2.4, and in the ten others, the photon indices range from 1.6 to 1.9–2.1.

- Soft excess components are often present in the spectra of NLS1s. In comparison, they are not often seen in the *ASCA* spectra of Seyferts with broader optical lines [9]. The soft excess can generally be recognized as positive residuals when a spectral fit above 2 keV with a power law plus Galactic absorption model is extrapolated toward toward lower energies (Figure 2). A soft component was required in addition to the power law model to fit the spectra of 15 objects adequately. However, the size of the soft excess relative to the power law varies (Figure 2). The rest frame temperature of a black body model is in the range 100–200 eV.

- Absorption is not commonly found in the spectra of NLS1s. In this sample of 21 objects, absorption is clearly observed in 6 objects, and is marginally detected in 1 other. Of the 6 spectra, the absorbing material is clearly ionized in 4, and may be ionized in the other 2. The situation is different for objects with broader optical lines; for example, Reynolds (1996) found evidence for ionized absorption in 12 of 24 objects [9]. Selection effects may bias the results, however. Many of Reynold's targets are hard X-ray selected and therefore are picked up regardless of low to moderate absorption columns. In contrast, many of the NLS1s considered here are either optically selected or soft X-ray selected, and therefore large absorption columns are selected against. Furthermore, it is difficult to detect moderate or weak absorption in poor signal-to-noise *ASCA* spectra when there is also a soft excess.
- Because of the steep spectra and often low flux, it is in general difficult to obtain interesting constraints on the iron line parameters from NLS1s. A relativistic disk line was found in the spectrum of NGC 4051 [10]. Iron lines with energy consistent with neutral iron are found in Mrk 335 and Mrk 766. In Ton S180, the energy of the iron line is characteristic of ionized iron [8]; this result was also found in the *BeppoSAX* spectrum from this object [11].
- Three NLS1s show absorption features near 1 keV in their soft X-ray spectra. These were interpreted as blue-shifted oxygen absorption edges or lines in relativistically outflowing gas [12]. This interpretation is supported by the fact that NLS1s and low ionization broad absorption line quasars (BALQSOs) share several optical emission line and broad band continuum properties.
- Three NLS1s show emission features near 1 keV. In the case of PG 1244+026, this was interpreted as emission from photoionized iron and neon [13].

REFERENCES

1. Goodrich, R. W., 1989, ApJ, 342, 224
2. Osterbrock, D. E. & Pogge, R. W. 1985, ApJ, 297, 166
3. Boller, Th., Brandt, W. N. & Fink, H., 1996, A&A, 305, 53
4. Laor, A. et al. 1997, ApJ, 477, 93
5. Forster, K. & Halpern, J. P. 1996, ApJ, 468, 565
6. Nandra, K., et al., 1997, ApJ, 476, 70
7. Leighly, K. M., Kay, L. E., Wills, B. J., Wills, D., & Grupe, D., 1997, ApJL, 489, 137
8. Leighly, K. M., et al. 1997, in prep.
9. Reynolds, C. S., 1997, MNRAS, 286, 513
10. Guainazzi, M., Mihara, T., Otani, C., & Matsuoka, M., 1996, PASJ, 48, 781
11. Comastri, A., et al. 1997, A& A, in press
12. Leighly, K. M., Mushotzky, R. F., Nandra, K., & Forster, K., 1997, ApJL, 489, 25
13. Fiore, F., et al. 1997, MNRAS, in press

THE ASTROPHYSICAL JOURNAL, 489:L25–L28, 1997 November 1

EVIDENCE FOR RELATIVISTIC OUTFLOWS IN NARROW-LINE SEYFERT 1 GALAXIES

KAREN M. LEIGHLY
Columbia Astrophysics Laboratory, 538 West 120th Street, New York, NY 10027; leighly@ulisse.phys.columbia.edu
RICHARD F. MUSHOTZKY
Goddard Space Flight Center, Code 660.2, Greenbelt, MD 20770; mushotzky@lheavx.gsfc.nasa.gov
KIRPAL NANDRA[1]
Goddard Space Flight Center, Code 660.2, Greenbelt, MD 20770; nandra@lheavx.gsfc.nasa.gov
AND
KARL FORSTER
Department of Astronomy, Columbia University, 538 West 120th Street, New York, NY 10027; karlfor@mikado.columbia.edu
Received 1997 April 30; accepted 1997 August 11; published 1997 October 7

ABSTRACT

We report the observation of features near 1 keV in the *ASCA* spectra from three narrow-line Seyfert 1 (NLS1) galaxies. We interpret these as oxygen absorption in a highly relativistic outflow. If interpreted as absorption edges, the implied velocities are 0.2–0.3 c, near the limit predicted by "line-locking" radiative acceleration. If instead interpreted as broad absorption lines, the implied velocities are ~0.57 c, interestingly near the velocity of particles in the last stable orbit around a Kerr black hole, although a physical interpretation of this is not obvious. The features are reminiscent of the UV absorption lines seen in broad absorption line quasars (BALQSOs), but with larger velocities, and we note the remarkable similarities in the optical emission line and broadband properties of NLS1s and low-ionization BALQSOs.

Subject headings: galaxies: active — galaxies: individual (IRAS 13224−3809, 1H 0707−495, PG 1404+226) — X-rays: galaxies

1. INTRODUCTION

Narrow-line Seyfert 1 galaxies (NLS1s) are defined by their optical line properties (see, e.g., Goodrich 1989): (1) the Balmer lines are only slightly broader than the forbidden lines (Hβ FWHM < 2000 km s^{-1}); (2) the forbidden line emission is relatively weak ([O III] λ5007/Hβ < 3); and (3) there are often strong emission features from Fe II and high-ionization optical lines. It has recently been discovered that they also have distinctive X-ray properties. *ROSAT* PSPC observations found that the soft X-ray spectra are systematically steeper than in "classical" Seyfert 1 galaxies and that the photon index appears correlated with the optical line width. NLS1s also very frequently exhibit rapid and/or high-amplitude X-ray variability (Boller, Brandt, & Fink 1996; Forster & Halpern 1996 and references therein).

NLS1 observations with *ASCA*, which has better energy resolution and a larger bandpass, find that the steep spectrum in the soft X-ray band is primarily due to a strong soft excess component with characteristic blackbody temperature in the range 0.1–0.2 keV and a relatively weak hard power law. The hard X-ray power-law slope is either remarkably variable (Leighly et al. 1996; Guainazzi et al. 1996) or significantly steeper than found in broad-line Seyfert 1 galaxies (Pounds, Done, & Osborne 1995; Brandt, Mathur, & Elvis 1997). The combination of strong soft excess and steep power law prompted Pounds et al. (1995) to postulate that NLS1s represent the supermassive black hole analog of Galactic black hole candidates in the high state.

2. DATA AND ANALYSIS

We considered all the *ASCA* data from NLS1s in the archive as of 1997 February and in three proprietary data sets, yielding a sample of 16 objects. A standard uniform analysis was applied to all data (see, e.g., Nandra et al. 1997; details in Leighly et al. 1997).

In most cases, a power-law model fitted the spectra poorly, and an additional soft excess model was required. The soft component in these NLS1s is hot and prominent, and a single blackbody is not broad enough to fit the whole energy range from 0.48 keV. A disk blackbody model, which is the sum of blackbodies (Makishima et al. 1986), is broader. Therefore, we fitted a disk blackbody model in the energy band greater than 0.48 keV. However, our discussion of absorption features below does not depend critically on the assumed model of the soft continuum. Fits over a truncated energy band of more than 0.6 keV with a single blackbody give consistent parameters for the absorption features, with comparable χ^2_ν values.

In many cases, the power-law plus disk blackbody model gave an adequate fit. However, a significant dip remained near 1 keV in the fit residuals from 1H 0707−495, IRAS 13224−3809, and PG 1404+226 (Fig. 1; also see Hayashida 1996; Otani, Kii, & Miya 1996; Comastri, Molendi, & Ulrich 1997). Similar features have been reported in *ROSAT* spectra from Akn 564 (Brandt et al. 1994) and PG 1404+226 (Ulrich-Demoulin & Molendi 1996). Addition of an edge to the model improved the fit by $\Delta\chi^2$/degrees of freedom (d.o.f.) = 33/265, 46/307, and 35/156, significant at a confidence level greater than 99.9%, for 1H 0707−495, IRAS 13224−3809, and PG 1404+226, respectively. For 1H 0707−495 and IRAS 13224−3809, an additional edge reduced the χ^2 by 24 and 11, respectively. The best-fit parameters for these two-edge fits and the single-edge fit for PG 1404+226 are listed in Table 1.

Absorption edges, a signature of highly ionized gas in the line of sight, are commonly found in the X-ray spectra from bright Seyfert 1 galaxies (see, e.g., Reynolds 1997). Oxygen edges from O VII and O VIII at 0.74 and 0.87 keV, respectively, are expected to dominate the absorption profile because of the

[1] National Academy of Science/National Research Council research associate.

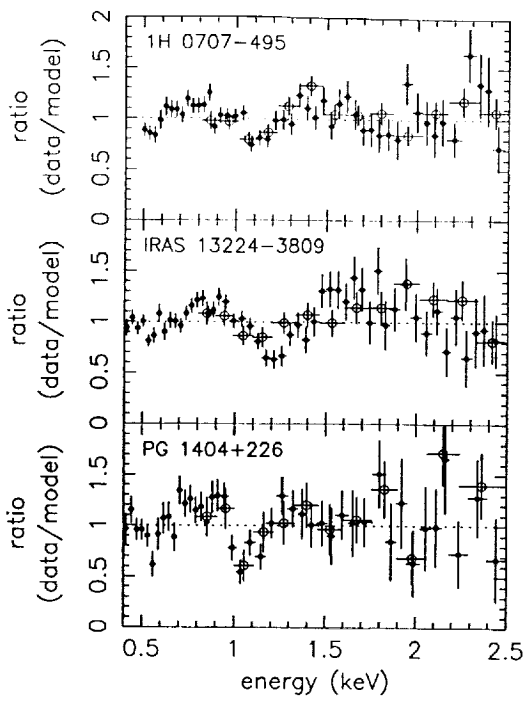

FIG. 1.—Ratio of data to a power-law plus disk blackbody model, showing the edge-like feature around 1 keV in these three objects. Filled and open symbols denote summed SIS and GIS spectra, respectively.

large abundance and cross sections. However, the edges in our objects are found at much higher energies than could be attributed to oxygen in the active galactic nucleus (AGN) rest frame. In this energy range, absorption by neon and iron is expected, but for abundances near solar value, it is difficult to produce deep absorption edges from these elements without also finding strong oxygen edges. Since neon differs in atomic number from oxygen by only two, its ionization state should not be drastically different. Since both oxygen and neon are plausibly produced predominately by Type II supernovae, their relative abundances should not vary much. Iron species that could absorb from the L shell are still present when oxygen is nearly fully ionized, but the expected dominant ions have higher energy absorption edges than we find here, near 1.2–1.4 keV.

We can attribute the absorption edges to ionized oxygen if the absorbing material is being accelerated away from the nucleus, similar to broad absorption line galaxies (BALQSOs; for recent reviews, see Weymann 1995; Turnshek 1995). If we identify the observed edges in 1H 0707−495 and IRAS 13224−3809 with O VII and O VIII, we infer an ejection velocity of about -0.2 to -0.3 c (Fig. 2*a*). This interpretation is supported by the consistency in velocity for both ions. For PG 1404+226, we detect only one edge and infer velocity of either -0.35 or -0.20 c, depending on whether it is due to O VII or O VIII.

Alternatively, the absorption features may be due to resonance line absorption. The *ASCA* SIS detectors have moderate resolution (~60 eV at 1 keV), and since the lines have a low equivalent width of ~50 eV, they can be detected only if the velocity dispersion is $\sigma_{vel} \gtrsim 3000$ km s^{-1}. We added "narrow" ($\sigma = 0$) Gaussian lines to the power-law plus disk blackbody model, effectively modeling features narrower than the detector response width. Addition of an absorption line to the disk blackbody plus power-law model reduced the χ^2/d.o.f. by 30/265, 25/303, and 21/151 and the second line by 15/263, 6/301, and 14/149 for 1H 0707−495, IRAS 13224−3809, and PG 1404+226, respectively. Addition of a third line for 1H 0707−495 and IRAS 13224−3809 reduced the χ^2/d.o.f. by 20/261 and 5/298. Details of these multiple-line fits are shown in Table 1. The final χ^2 values are comparable to the edge fit

TABLE 1

SPECTRAL FITTING RESULTS

TARGET	N_H[a] (10^{21} cm^{-2})	POWER LAW		BLACKBODY		ABSORPTION FEATURE[b]			χ^2/d.o.f.
		Index	Norm.[c]	kT (keV)	Norm.[d]	Energy (keV)	Depth	ID[e]	
Absorption-Edge Model									
1H 0707−495	$0.63^{+0.71}_{-0.05}$	$2.29^{+0.22}_{-0.21}$	$6.0^{+1.9}_{-1.4}$	$0.20^{+0.02}_{-0.03}$	$0.26^{+0.64}_{-0.09}$	$0.91^{+0.03}_{-0.04}$	0.57 ± 0.20	O VII	318/263
						1.09 ± 0.03	0.67 ± 0.23	O VIII	
IRAS 13224−3809	$0.48^{+0.63}_{-0}$	$1.97^{+0.26}_{-0.25}$	$2.05^{+0.74}_{-0.55}$	$0.19^{+0.02}_{-0.03}$	$0.18^{+0.49}_{-0.07}$	1.03 ± 0.04	$0.60^{+0.28}_{-0.25}$	O VII	339/300
						$1.18^{+0.04}_{-0.03}$	$0.87^{+0.31}_{-0.32}$	O VIII	
PG 1404+226	$0.55^{+1.67}_{-0.34}$	1.67 ± 0.42	$1.5^{+1.1}_{-0.7}$	$0.18^{+0.04}_{-0.05}$	$0.22^{+4.0}_{-0.15}$	1.07 ± 0.03	$1.15^{+0.41}_{-0.44}$	O VII or O VIII	153/151
Absorption-Line Model									
1H 0707−495	1.6 ± 0.08	2.25 ± 0.18	$5.9^{+1.4}_{-1.2}$	0.15 ± 0.02	$2.5^{+6.5}_{-1.8}$	0.98 ± 0.03	30^{+20}_{-15}	N VII	319/261
						$1.12^{+0.03}_{-0.02}$	47^{+18}_{-17}	O VII	
						1.24 ± 0.03	46 ± 20	O VIII	
IRAS 13224−3809	$2.3^{+1.1}_{-0.9}$	1.89 ± 0.23	$1.80^{+0.57}_{-0.46}$	0.13 ± 0.02	$5.3^{+22.2}_{-4.1}$	$1.09^{+0.05}_{-0.03}$	24^{+18}_{-17}	O VII	343/298
						1.23 ± 0.04	48^{+19}_{-24}	O VIII	
						$1.33^{+0.06}_{-0.05}$	46^{+29}_{-31}	?	
PG 1404+226	$2.3^{+1.4}_{-1.2}$	1.68 ± 0.33	$1.53^{+0.75}_{-0.54}$	$0.13^{+0.03}_{-0.02}$	$4.8^{+34.0}_{-4.0}$	1.12 ± 0.03	50^{+29}_{-25}	O VII	150/149
						1.24 ± 0.04	51^{+30}_{-22}	O VIII	

NOTE.—The quoted uncertainties are 90% confidence for two parameters of interest ($\Delta\chi^2 = 4.61$).

[a] Neutral continuum absorption. The lower limit is the Galactic absorption column for the edge fits.

[b] Absorption feature depths are the optical depth τ and the line equivalent width in eV for the edge and line models, respectively. Listed on successive lines are parameters for models with more than one absorption feature.

[c] In units of 10^{-4} photons cm^{-2} s^{-1} at 1 keV.

[d] Multiple blackbody model (Makishima et al. 1986) times $10^{17}(R_{IS}/D_{10})^2 \times \cos(\theta)$, where R_{IS} is the inner disk radius in kilometers, D is the distance to the source in units of 10 kpc, and θ is the disk inclination.

[e] Tentative edge/line identification, implying velocities in Fig. 2.

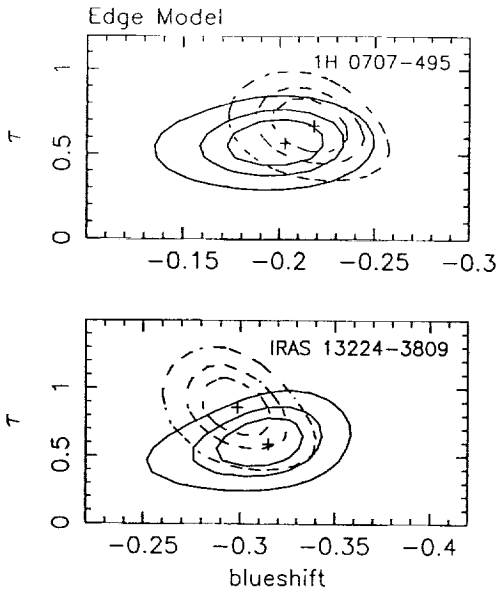

FIG. 2a

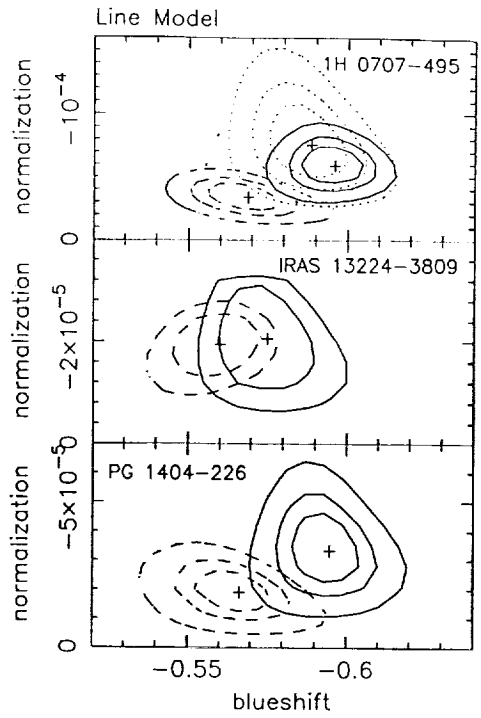

FIG. 2b

FIG. 2.—When the edges and lines are identified with transitions of oxygen, the ejection velocities from the nucleus can be found. χ^2 contours show 67%, 90%, and 99% confidence intervals; for IRAS 13224−3809, only 67% and 90% confidence are shown. (*a*) Absorption-edge fits; (*b*) absorption-line fits. Solid, dashed, and dotted lines indicate O VII, O VIII, and N VI, respectively.

results, so we cannot distinguish these models statistically. Note that the two lines present in all spectra are consistent in energy from object to object, although the differences in cosmological redshift (z = 0.041, 0.067, and 0.098 for 1H 0707−495, IRAS 13224−3809, and PG 1404+226, respectively) imply a difference of 50 eV in observed energy. Assuming that the absorber is completely opaque and fitting with the XSPEC *notch* model (equivalent to a very saturated absorption line) gives a velocity profile FWHM of ~10,000–14,000 km s^{-1}, similar to that found in BALQSOs. Resonance absorption is expected to be strong in hydrogen-like and helium-like atoms, and the ratios of the energies should be the same for every element. Again, we can plausibly identify the two common lines in all spectra as O VII and O VIII at ~0.565 and 0.651 keV, respectively. A lower energy line in the 1H 0707−495 spectrum is plausibly N VII at 0.498 keV, while a higher energy line in the IRAS 13224−3809 spectrum has no clear identification. These line identifications imply consistent ejection velocities, near −0.57 c (Fig. 2*b*). Absorption edges should accompany the resonance absorption lines (Madejski et al. 1993). Adding O VII and O VIII absorption edges to the model with energies fixed at the values predicted if $v/c = -0.57$, we find that the optical depths τ are consistent with zero, and the $\Delta\chi^2 = 4.61$ upper limits were 0.27, 0.68, and 0.50 for O VII and 0.32, 0.13, and 0.26 for O VIII, for 1H 0707−495, IRAS 13224−3809, and PG 1404+226, respectively. In § 3 we show that estimations of the column densities derived from these upper limits are consistent with those from the absorption-line equivalent widths.

As noted above, the measured edge energies seem inconsistent with those expected from iron-L species. However, iron is a complex ion potentially producing a complex absorption profile that might fit these moderate-resolution spectra. We used a power-law plus disk blackbody model, transmitted through an ionized absorber in the AGN rest frame with iron abundance free (Magdziarz & Zdziarski 1995). In this model, the electron temperature T and the ionization parameter ξ are both free parameters, and we chose two representative values, $T_{\rm low} = 3 \times 10^4$ K and $T_{\rm high} = 3 \times 10^5$ K. These models produced a worse fit overall compared with the models described above and required rather large iron overabundances. For $T = T_{\rm low}$, we obtained iron abundance lower limits of 15, 29, and 17 times solar values with $\Delta\chi^2$/d.o.f. = 11/264, 13/301, and 6/150, and for $T = T_{\rm high}$, we obtained iron abundance best-fit values of 3.9, 7.3, and 12.8 with $\Delta\chi^2$/d.o.f. = 0/264, 12/301, and 7/150 for 1H 0707−495, IRAS 13224−3809, and PG 1404+226, respectively. Iron enhancements up to 10 with respect to oxygen might be expected in some cases, but probably not as large as 20 (Hamann & Ferland 1993). A high iron abundance could not be responsible for the strong Fe II emission in NLS1s, because the resulting cooler temperature decreases the number of Fe^+ ions while the optical depth to escaping Fe II increases (see, e.g., Joly 1993).

In summary, we tried to explain the 1 keV features using three different models. Both absorption edges and lines produced a good fit that could not be distinguished statistically. The iron overabundance model generally gave a poorer fit.

3. DISCUSSION

The outflow velocities of 0.2–0.6 c inferred in these objects are very large, larger than those observed the UV spectra of BALQSOs. Such large velocities could be difficult to identify in the UV band, because the prominent C IV line would be shifted out of the bandpass or into the Lyα forest, where it might be hard to distinguish. Also, very large velocity disper-

sions with moderate column densities might result in lines so broad that they blend in with the continuum.

It is beyond the scope of this Letter to speculate on the mechanism required to accelerate material to these very large velocities, but it is interesting to note that the velocity implied by the edge fits is close to that seen in the Galactic jet object SS 433 of 0.26 c and to the terminal velocity predicted by "line locking" of 0.28 c (Shapiro, Milgrom, & Rees 1986). The larger velocities implied by the absorption-line fits are intriguingly close to the energy of a particle in circular orbits around a Kerr black hole (see, e.g., Shapiro & Teukolsky 1983). However, it seems difficult to relate this fact to a physical outflow mechanism.

We obtain lower limits on the equivalent hydrogen column. For the absorption-edge model, assuming cross sections of 2.8 and 0.98 $\times$ 10^{-19} cm^{-2} for O VII and O VIII, respectively, and an oxygen abundance relative to hydrogen of 8.51 $\times$ 10^{-4}, the O VII+O VIII equivalent hydrogen column densities are in the range of 0.4–1.3 $\times$ 10^{22} cm^{-2}. For the absorption lines, assumed to be on the linear part of the curve of growth, oscillator strengths of 0.694 and 0.416 for O VII and O VIII were used, giving O VII+O VIII equivalent hydrogen column densities of 1.6–2.1 $\times$ 10^{21} cm^{-2}. In each case, the column density upper limits on the absorption edges predicted to accompany these absorption lines were larger, which shows that this model is viable. While estimation of the ionization parameter depends on the input continuum and is beyond the scope of this Letter, we note that the O VIII column is always larger than the O VII column, which implies a fairly high ionization parameter.

Rest-frame absorption features in the X-ray spectra of broad-line hard X-ray–selected AGNs are common (Reynolds 1997), plausibly arising in the same material as $z_{em} \approx z_{ab}$ absorption lines found in the UV band (see, e.g., Mathur, Elvis, & Wilkes 1995). These "associated" absorption features may be related to the broad UV absorption lines seen in higher luminosity objects (see, e.g., Kolman et al. 1993). Evidence suggests that some aspect of the NLS1 central engine is significantly different compared with broad-line objects; for example, they may be characterized by a higher accretion rate relative to Eddington luminosity (Pounds et al. 1995). The rapid, higher amplitude, and perhaps characteristically nonlinear X-ray variability may be evidence for strong relativistic effects (Boller et al. 1997; Leighly et al. 1997). These results may indicate a higher level of activity relative to the black hole mass in NLS1s, and strong relativistic outflows might be expected.

The blueshifted absorption features discussed here are reminiscent of those found in the UV spectra of broad absorption line quasars. A connection between NLS1s and BALQSOs may be quite reasonable, considering that they have many optical emission line and broadband continuum properties in common. Many NLS1s and BALQSOs show strong or extreme Fe II emission and weak [O III] emission. Objects that have the strongest Fe II emission and weakest or no [O III] emission tend to be either low-ionization BALQSOs or NLS1s (Boroson & Meyers 1992; Turnshek et al. 1997; Lawrence et al. 1997). Many NLS1s and low-ionization BALQSOs have red optical continuum spectra and relatively strong infrared emission (Boroson & Meyers 1992; Moran, Halpern, & Helfand 1996; Turnshek 1997). Finally, both classes are predominantly radio quiet (Stocke et al. 1992; Ulvestad, Antonucci, & Goodrich 1995).

An interesting possibility is that low-ionization BALQSOs and NLS1s have a common parent population (see, e.g., Lawrence et al. 1997). If so, perhaps objects with intermediate properties between NLS1s and low-ionization BALQSOs should exist. It was recently reported that NLS1 IRAS 13349+2438 has UV broad absorption lines (Turnshek 1997). But while most BALQSOs are X-ray quiet, this object is a bright soft X-ray source and has the very steep hard X-ray spectrum and rapid X-ray variability characteristic of NLS1s (Brinkmann et al. 1996).

K. M. L. acknowledges many enlightening discussions with Jules Halpern and helpful advice from Tim Kallman. K. M. L. gratefully acknowledges support through NAG5-3307 (*ASCA*). K. N. thanks the NRC for support.

REFERENCES

Boller, Th., Brandt, W. N., Fabian, A. C., & Fink, H. 1997, MNRAS, 289, 393
Boller, Th., Brandt, W. N., & Fink, H. 1996, A&A, 305, 53
Boroson, T. A., & Meyers, K. A. 1992, ApJ, 397, 442
Brandt, W. N., Fabian, A. C., Nandra, K., Reynolds, C. S., & Brinkmann, W. 1994, MNRAS, 271, 958
Brandt, W. N., Mathur, S., & Elvis, M. 1997, MNRAS, 285, 25
Brinkmann, W., Kawai, N., Ogasaka, Y., & Siebert, J. 1996, A&A, 316, 9
Comastri, A., Molendi, S., & Ulrich, M. H. 1997, X-Ray Imaging and Spectroscopy of Cosmic Hot Plasmas, ed. F. Makino & K. Mitsuda (Tokyo: Univ. Acad. Press), 279
Forster, K., & Halpern, J. P. 1996, ApJ, 468, 565
Goodrich, R. W. 1989, ApJ, 342, 224
Guainazzi, M., Mihara, T., Otani, C., & Matsuoka, M. 1996, PASJ, 48, 781
Hamann, F., & Ferland, G. 1993, ApJ, 418, 11
Hayashida, K. 1996, IAU Colloq. 159, Emission Lines in Active Galaxies: New Methods and Techniques, ed. B. M. Peterson, F.-Z. Cheng, & A. S. Wilson (San Fransisco: ASP), 40
Joly, M. 1993, Ann. Phys., 18, 241
Kolman, M., Halpern, J. P., Martin, C., Awaki, H., & Koyama, K. 1993, ApJ, 403, 592
Lawrence, A., Elvis, M., Wilkes, B. J., McHardy, I., & Brandt, N. 1997, MNRAS, 286, 879
Leighly, K. M., Mushotzky, R. F., Yaqoob, T., Kunieda, K., & Edelson, R. 1996, ApJ, 469, 14
Leighly, K. M., et al. 1997, in preparation
Madejski, G. M., et al. 1993, in BBXRT: A Preview to Astronomical X-Ray Spectroscopy in the '90s, ed. P. J. Serlemitsos, & S. Shrader (Greenbelt: NASA/GSFC), 63
Magdziarz, P., & Zdziarski, A. A. 1995, MNRAS, 273, 837
Makishima, K., et al. 1986, ApJ, 308, 635
Mathur, S., Elvis, M., & Wilkes, B. 1995, ApJ, 452, 230
Moran, E. C., Halpern, J. P., & Helfand, D. J. 1996, ApJS, 106, 341
Nandra, K., George, I. M., Mushotzky, R. F., Turner, T. J., & Yaqoob, T. 1997, ApJ, 476, 70
Otani, C., Kii, T., & Miya, K. 1996, in MPE Rep. 263, Röntgenstrahlung from the Universe, ed. H. U. Zimmermann, J. Trümper, & H. Yorke, 491
Pounds, K. A., Done, C., & Osborne, J. 1995, MNRAS, 277, L5
Reynolds, C. S. 1997, MNRAS, 286, 513
Shapiro, P. R., Milgrom, M., & Rees, M. J. 1986, ApJS, 60, 393
Shapiro, S. L., & Teukolsky, S. A. 1983, Black Holes, White Dwarfs, and Neutron Stars (New York: Wiley)
Stocke, J. T., Morris, S. L., Weymann, R. J., & Foltz, C. B. 1992, ApJ, 396, 487
Turnshek, D. A. 1995, in QSO Absorption Lines, ed. G. Meylan (Berlin: Springer), 223
———. 1997, in Mass Ejection from Active Galactic Nuclei, ed. R. J. Weyman, N. Arav, & I. Shlosman (San Francisco: ASP), in press
Turnshek, D. A., Monier, E. M., Sirola, C. J., & Espey, B. R. 1997, ApJ, 476, 40
Ulrich-Demoulin, M. H., & Molendi, S. 1996, ApJ, 457, 77
Ulvestad, J. S., Antonucci, R. R. J., & Goodrich, R. W. 1995, AJ, 109, 81
Weymann, R. J. 1995, in QSO Absorption Lines, ed. G. Meylan (Berlin: Springer), 213

THE ASTROPHYSICAL JOURNAL, 489:L137–L140, 1997 November 10

THE OPTICAL POLARIZATION AND WARM ABSORBER IN IRAS 17020+4544

KAREN M. LEIGHLY
Columbia Astrophysics Laboratory, 538 West 120th Street, New York, NY 10027; leighly@ulisse.phys.columbia.edu
LAURA E. KAY
Department of Physics and Astronomy, Barnard College, Columbia University, New York, NY 10027-6598
AND
BEVERLEY J. WILLS, D. WILLS, AND DIRK GRUPE
McDonald Observatory and Department of Astronomy, University of Texas at Austin, Austin, TX 78712
Received 1997 July 30; accepted 1997 September 10; published 1997 October 13

ABSTRACT

We report the detection of ionized absorption in the *ASCA* spectrum of the narrow-line Seyfert 1 galaxy IRAS 17020+4544. Subsequent optical spectropolarimetry revealed high polarization increasing from 3% in the red to 5% in the blue, which indicates electron or dust scattering as a likely origin. The broad emission line Hα is somewhat less polarized than the continuum, which supports a location of the polarizing material within the active galactic nucleus. The Balmer line decrement and reddened optical spectrum support the presence of a dusty warm absorber in this object.

We compared the broadband optical polarization and ionized X-ray absorption of a collection of Seyfert 1 and 1.5 galaxies, excluding classes of objects that are likely to have significant neutral X-ray absorption. Warm absorber objects are generally more likely to have high optical polarization than objects with no detected ionized absorption. This result lends additional support to the idea that the warm absorber is associated with dust and implies either that dust transmission is responsible for at least part of the polarization or that the polarization is revealed because of the dimming of the optical spectrum. Spectropolarimetry of Seyfert 1 galaxies generally locates the scattering material inside the narrow-line region and often close to or within the broad-line region, consistent with estimates of the location of the dusty warm absorber.

Subject headings: galaxies: active — galaxies: individual (IRAS 17020+4544) — galaxies: Seyfert — polarization — X-rays: galaxies

1. INTRODUCTION

ROSAT and *ASCA* observations of Seyfert 1 nuclei produced abundant evidence for highly ionized material in the line of sight. Signatures of the "warm absorber" are present in the X-ray spectra of about half of Seyfert 1 and 1.5 galaxies (Reynolds 1997). Recently, it was noticed that the warm absorber is often associated with optical reddening (Reynolds 1997; Brandt, Fabian, & Pounds 1996), which supports the idea that the warm absorber may coexist with dust. Dust reddens the UV-optical continuum spectrum, but it can also polarize it. Thus, one might expect high optical polarization in Seyfert 1 galaxies that show warm absorber features in their X-ray spectra. As part of an archival analysis program of *ASCA* data (Leighly et al. 1997), we discovered evidence for a warm absorber in the narrow-line Seyfert 1 galaxy IRAS 17020+4544. Noting that it also has a red optical spectrum, we strongly suspected that a dusty warm absorber would be present. To test the connection between warm absorbers and optical polarization, we obtained spectropolarimetry and confirmed high polarization.

2. DATA AND ANALYSIS

IRAS 17020+4544 is a member of the IRAS Point Source Catalog (IRAS PSC) and was originally classified as a Seyfert 2 with redshift of $z = 0.0602$ (De Grijp et al. 1992). The X-ray emission was first discovered in the cross-correlation between the *ROSAT* All-Sky Survey and the IRAS PSC (Boller et al. 1992). Subsequent higher resolution spectroscopy revealed Fe II lines and Hβ significantly broader than [O III] (Moran, Halpern, & Helfand 1996), which forced its reclassification as a narrow-line Seyfert 1 galaxy (NLS1; Osterbrock & Pogge 1985; Goodrich 1989b).

2.1. *X-Ray Spectral Analysis*

IRAS 17020+4544 was observed with *ASCA* on 1995 August 29, and the data were retrieved from the archive. Standard analysis procedures were followed (see, e.g., Nandra et al. 1997; for details, see Leighly et al. 1997), which resulted in approximately 33 ks of net exposure. The source was bright, about 0.49 counts s^{-1} in the SIS0. Since our primary interest is in the warm absorber, we report only analysis relevant to that here.

Preliminary fitting indicated spectral complexity in soft X-rays. We fitted a power-law plus a narrow iron line to the data above 2 keV, then extrapolated that fit to lower energies, including a neutral absorption column of $N_H = 3.5 \pm 0.5 \times 10^{20}$ cm^{-2} measured from the *ROSAT* PSPC spectrum; note that the Galactic column in this direction is 2.2×10^{20} cm^{-2} (Dickey & Lockman 1990). The residuals in Figure 1 show that the source is absorbed in soft X-rays, and there is an edge near 0.7 keV that is a characteristic signature of the warm absorber (see, e.g., Reynolds 1997). A power-law, narrow Gaussian (to model the iron Kα line), and additional absorption model over the whole range from 0.4–10.0 keV gives a poor fit with $\chi^2 = 1167$ for 971 degrees of freedom (d.o.f.). Addition of an absorption edge improves the fit significantly ($\Delta\chi^2 = -131$ for 2 additional d.o.f.). The edge energy is 0.71 ± 0.02 keV (errors are 90% for one interesting parameter), roughly consistent with O VII absorption. Addition of another edge gives no improvement in fit. Following Reynolds (1997) by fixing the two edge energies at 0.74 and 0.87 keV corre-

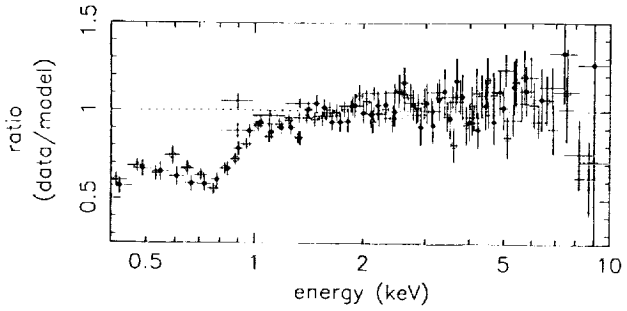

FIG. 1.—Ratio of a power-law plus absorption column obtained from *ROSAT* spectrum (3.5×10^{20} cm^{-2}, Galactic $N_H = 2.2 \times 10^{20}$ cm^{-2}) model fit above 2 keV and extrapolated to low energies. The open and filled circles correspond to the SIS0 and SIS1 spectra, respectively, while the crosses correspond to the GIS2 and GIS3 spectra.

sponding to O VII and O VIII results in a slightly worse fit than the single edge fit by $\Delta\chi^2 = 8$ with the optical depth of the O VIII edge equal to zero. This suggests that the ionization state of the warm absorber is somewhat low compared with those of objects studied by Reynolds (1997).

Next we model the warm absorber with the photoionization model Absori, available in XSPEC (Magdziarz & Zdziarski 1995). This model results in a somewhat poorer fit (χ^2/d.o.f. = 1071/969) than the edge model but provides an estimate of the ionized column density of $N_w = 2.5^{+0.6}_{-0.5} \times 10^{21}$ cm^{-2} and the ionization parameter $\xi = 9.5^{+19}_{-7.6}$. Evidence for emission around 1 keV remains in the residuals. This feature can be modeled as a marginally resolved line at 1.1 keV with an equivalent width of 75 eV, and then $N_w = 3.5^{+0.6}_{-0.5} \times 10^{21}$ cm^{-2}, $\xi = 6.1^{+9.8}_{-3.3}$, intrinsic $N_H = 5.5^{+2.1}_{-1.8} \times 10^{20}$ cm^{-2}, and χ^2/d.o.f. = 1016/967. The 1 keV feature may be similar to the emission features seen in the X-ray spectrum of other NLS1s, possibly a blend of photoionized iron and neon emission lines (e.g., PG 1244+026: Fiore et al. 1997; Ton S180 and Akn 564: Leighly et al. 1997).

2.2. *Spectropolarimetry*

We obtained spectropolarimetry data on IRAS 17020+4544 at the Lick Observatory 3 m telescope with the KAST spectrograph (see, e.g., Martel 1996) and at the McDonald Observatory 2.7 m telescope with the Large Cassegrain Spectrograph (see, e.g., Hines & Wills 1993). Figure 2 shows spectropolarimetry results. The polarization position angle is constant at about 166° and is therefore not shown. We measured the host galaxy axial ratio on the Digitized Sky Survey image to be 0.55 ± 0.02 with a position angle of $168° \pm 1°$, in good agreement with the polarization position angle. Broadband imaging polarimetry measurements with the McDonald Observatory 2.1 m telescope (Grupe et al. 1997) agree in position angle and in the blue but find lower polarization in the red, probably a result of a larger aperture (7".4 diameter compared with 2" slits). We find the following (filter, effective wavelength, and percentage polarization, respectively): U, 3600 Å, 7.1 ± 3.1; CuSO4, 4200 Å, 3.93 ± 0.35; none, 5700 Å, 2.42 ± 0.18; and RG 630, 7600 Å, 1.68 ± 0.20). The spectropolarimetry data indicate that the continuum is polarized at about 3% at the red end, increasing to 5% at the blue end. The Balmer lines of Hα (and perhaps Hβ) are less polarized than the continuum average, and the [N II] λλ6548, 6583 and [O III] λλ4959, 5007 lines may be slightly less polarized than the Balmer lines. In polarized flux

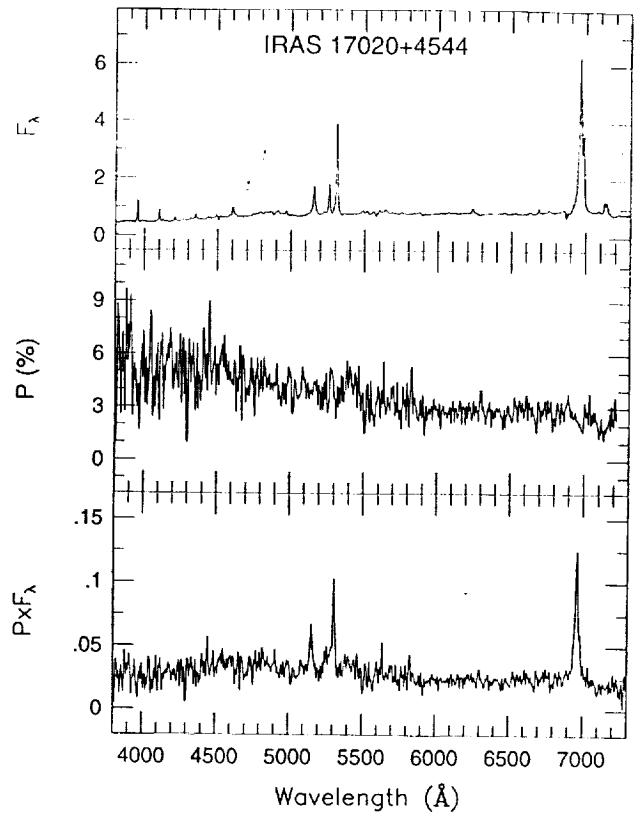

FIG. 2.—Spectropolarimetry of IRAS 17020+4544 uncorrected for reddening or redshift. The Lick data (60 minute exposure on 1997 March 8) were matched to the McDonald data (200 minutes exposure on 1997 April 8 and 10), taking into account small differences in polarization in the red, possibly the result of host galaxy starlight. The flux is in units of 10^{-15} ergs^{-1} s^{-1} cm^{-2} Å^{-1}. The second panel is the polarization (strictly Stokes q rotated to a position angle of 163°), and the third is the corresponding polarized flux. No other corrections were made, as lack of strong stellar absorption lines in the direct flux spectrum suggests little contamination.

the [O III]/Hβ ratio is lower than in direct flux, and the [N II] λ6583/Hα ratio may also be slightly lower. The direct and polarized flux widths are reasonably similar in Hα; this is probably true but more difficult to measure in Hβ. Since the widths of the Balmer lines are similar in polarized and direct flux, and the continuum polarization clearly rises to the blue, we can conclude that reflection by dust or electrons is a likely cause of the polarization, although dust transmission may contribute (see below). This is in agreement with a sample of NLS1s observed by Goodrich (1989b). We note also that high polarization is often found in dusty IRAS-selected active galactic nuclei (AGNs) (see, e.g., Wills & Hines 1997).

In direct flux, Hα/Hβ = 8.4. Following Reynolds et al. (1997), for a Galactic interstellar medium dust-to-gas ratio and assuming an intrinsic ratio of 3.1 (Veilleux & Osterbrock 1987), we derive 4.0×10^{21} cm^{-2} for the column density, roughly consistent with the ionized column density measured in the X-rays. This result supports the association of the dust with the ionized gas and suggests that the broad lines are seen through most of the obscuring screen. In polarized flux, Hα/Hβ was ~3.5; however, statistics were not good enough to measure the lines accurately. The polarized flux spectrum is nearly flat, as the reddening seen in the direct flux spectrum cancels the rise to the blue in polarization.

3. DISCUSSION

On the basis of the discovery of the warm absorber in IRAS 17020+4544, we postulated high polarization and found that it was present. We collected data from the literature to test the generality of the association between the presence of the warm absorber and high optical polarization.

The sample was chosen carefully. Because our goal was to test the association of the *ionized* absorber with optical polarization, we excluded objects in which high *neutral* columns are expected, since dust associated with the neutral column could also produce polarization. Therefore, we included Seyfert 1, 1.5, and narrow-line Seyfert 1 galaxies, but excluded Seyfert 1.8, 1.9, and narrow emission line galaxies (NELGs), which are often reddened, suffer X-ray absorption, and lie in galaxies viewed at a high inclination angle (Goodrich 1989a, 1995; Lawrence & Elvis 1982; Mushotzky 1982; Forster et al. 1997). We also excluded objects at low Galactic latitude to avoid polarization by the Galactic interstellar medium; nevertheless, this contributes a systematic error of about 0.3%–0.4%. Optical polarization of Seyfert 1 galaxies is correlated with the axial ratio of the host galaxy (Berriman 1989; Thompson & Martin 1988), so we exclude objects with low *b/a* (IC 4329a, Mrk 1040) unless differences in line and continuum polarization indicate that the absorber is inside the AGN (3A 0557−383: Brindle et al. 1990b). Broad-line radio galaxies are also excluded, since a contribution to their polarization may come from a nonthermal component (Rudy et al. 1983; Antonucci 1984), and they also sometimes show weak intrinsic neutral X-ray absorption (Woźniak et al. 1997).

The resulting sample comprised all the objects from Reynolds (1997) excluding those listed above, MR 2251-178, for which we found no polarization measurement, and 3C 273. We included Mrk 766 (Leighly et al. 1996), IRAS 13349+2438 (Brandt et al. 1997), 3A 0557−385 (Turner, Netzer, & George 1996), and NGC 7213 (Otani 1996) and Akn 120, I Zw 1, Mrk 478, Mrk 279, and Mrk 110 (from the archive and analyzed by K. M. L. following § 2.1 and Reynolds 1997; warm absorbers were not detected in these objects). Broadband polarization measurements in the band 3800–5600 Å, which is blue enough to minimize dilution by cool starlight, were used. The values were taken predominantly from Berriman (1989), except for Mrk 766 (Goodrich 1989b), IRAS 13349+2438 (average of *B* and *V* bands; Wills et al. 1992), Mrk 335 and Mrk 110 (Berriman et al. 1990), and IRAS 17020+4544 (presented here).

The polarization versus column density is shown in Figure 3. Open circles mark the ionized absorber column density in objects in which a warm absorber was detected, while filled circles plot the excess neutral column density over Galactic column density in objects with no detectable warm absorbers. Objects with no measurable excess neutral column are assigned $N_H = 1 \times 10^{20}$ cm^{-2}, approximately the level of systematic error from *ASCA* spectra, and errors equal to max{fit upper limit, 1×10^{20} cm^{-2}}. The neutral column density of the warm absorber objects is not taken into account, since the warm column density is very much larger than the cold column density in all cases except 3A 0557−383. This plot shows that objects with high optical polarization ($\gtrsim$1%) are very likely to have warm absorbers. However, the converse is not generally true; i.e., objects with high ionized columns do not necessarily have high optical polarization. Two notable examples, NGC 3783 and NGC 3516, are discussed below. Note that scatter is expected since the warm absorber can in principle respond rapidly to ionizing flux changes while dust properties are expected to change on much longer timescales. Nevertheless, the KS test indicates a different distribution of polarization of warm and cold absorber objects with 99% confidence.

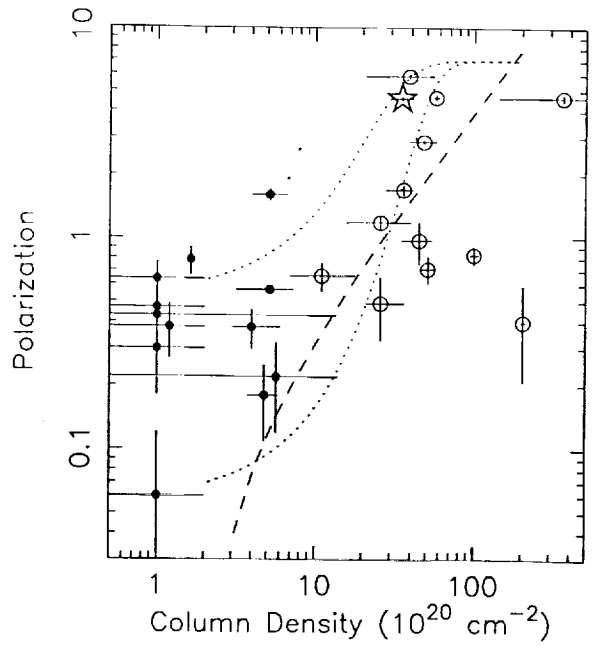

FIG. 3.—Absorption column vs. polarization. *Open circles*: ionized column density of objects with warm absorbers detected in *ASCA* spectra; *filled circles*: excess neutral absorption over Galactic absorption in objects with no detectable warm absorber (see text). The star marks the position of IRAS 17020+4544. *Dashed curve*: predicted maximum polarization from dust transmission. *Dotted curves*: predicted polarization from scattering assuming 7% intrinsic polarization and two assumed ratios of scattered to direct flux: 0.1 and 0.01 for upper and lower curves, respectively.

Brandt et al. (1996) first speculated that the high degree of optical reddening in IRAS 13349+2438 could be reconciled with the bright soft X-ray emission only if the gas associated with the dust responsible for reddening were ionized. Reynolds (1997) found a strong relationship between the reddening of the optical spectrum and the optical depth of the ionized absorber O VII edge in a sample of 24 AGNs. In a sample of bright soft X-ray–selected objects, Grupe et al. (1997) found that significant polarization occurred in objects in which the degree of optical reddening was too high to be consistent with the relatively unabsorbed soft X-ray spectra unless the gas were ionized. These results all support the association of the warm absorber with dust.

Generally speaking, in Seyfert 1 and 1.5 galaxies, the narrow emission lines are less polarized than the broad lines, which are in turn less polarized than the continuum, indicating that the scattering material is interior to the narrow-line region (NLR). Many Seyfert 1 and 1.5 galaxies show changes in position angle across the broad emission lines (see, e.g., Goodrich & Miller 1994; Martel 1996) and variability in the polarization properties on timescales of months to years (Martel 1996; Smith et al. 1997), indicating that the scattering region is not much larger than the broad-line region (BLR). If the dust is associated with the warm absorber, it must be located far enough from the nucleus that the dust does not evaporate. MCG −6-30-15 apparently has an inner and outer warm absorber (Otani et al. 1996), and it is probable that the outer one is dusty (Reynolds et al. 1997). Since it is unlikely that the dust could condense

out of ionized gas, a source of dusty gas that can then be ionized is required; this could be a wind off the molecular torus lying at a radius between the BLR and NLR radii in unified models (Reynolds et al. 1997). It has been suggested that dust absorption may naturally result in a line-free zone between the BLR and NLR (Netzer & Laor 1993). The narrow "associated" UV absorption lines may originate in warm absorber material (see, e.g., Mathur, Elvis, & Wilkes 1995); since these are superposed on the broad emission lines, a location outside the BLR is required. These results all support a similar location for the polarizing material and the dusty warm absorber.

The warm absorber measures conditions in line-of-sight gas. If the same material is responsible for the warm absorber, reddening, and polarization, then dust transmission must be responsible for at least part of the polarization. The dashed line in Figure 3 shows the predicted polarization versus column density for the dust transmission mechanism. We assumed the empirical laws appropriate for the Galactic interstellar medium (Clayton & Cardelli 1988), including a maximum polarization of $P_{max} = 9\% E(B - V)$, a ratio of total-to-selective extinction of $R_V = 3.1$, and the N_H-to-reddening relation from Heiles, Kulkarni, & Stark (1981). Polarization should lie below this line if dust transmission is the only polarizing mechanism. However, dust and electron scattering may also contribute to the polarization; furthermore, the geometry, grain alignment, dust composition, and dust-to-gas ratio are probably different in the AGN. Another possibility is that high polarization is revealed as a consequence of the suppression of the unpolarized direct (rather than scattered) light by reddening (see, e.g., Wills et al. 1992). The dotted lines in Figure 3 show the predicted polarization versus N_H for this model. We assumed that the intrinsic maximum polarization is 7%, seen when the direct continuum is completely attenuated, and that the ratio of scattered to direct light is 0.1 or 0.01 (upper and lower curves, respectively).

While NGC 3516 and NGC 3783 have among the highest ionized column densities ($N_w = 100$ and 204×10^{20} cm^{-2}), they have only moderate polarization (~0.83% and ~0.40%, respectively) and are not substantially reddened (Reynolds 1997). Perhaps only the inner warm absorber is present or the dust has been destroyed in these objects. Electron scattering could be the origin of the moderate polarization. No strong wavelength dependence is seen in either object, consistent with this idea (NGC 3516: Martel 1996; NGC 3783: Brindle et al. 1990a, 1990b). Goodrich & Miller (1994) find that a maximum of 7% polarization can be obtained in Seyfert 1 galaxies when the optical depth is $\tau = 1$. The ionized column densities present an optical depth of $\tau = 0.1$, and therefore the observed polarization could be consistent with an origin of scattering by free electrons in the ionized gas.

It would be interesting to extend this work to include Seyferts with significant neutral absorption: Seyfert 1.8 and 1.9 galaxies and NELGs. All together, this may support a picture in which the dust, ionized gas, and broad emission line clouds have a common origin in Seyfert 1 galaxies and intermediate-type Seyferts, with a decreasing inclination angle reducing the amount of obscuring material in the line of sight but revealing gas of increasing ionization parameter.

The authors thank Ross Cohen for contributing the Lick observing time. K. M. L. thanks R. Mushotzky for useful comments on a draft. K. M. L., L. E. K., B. J. W., and D. G. gratefully acknowledge support through NAG5-3307 (*ASCA*), NSF career grant Ast 9501835, GO-06766 (STScI), and NAG5-3431 (LTSA).

REFERENCES

Antonucci, R. R. J. 1984, ApJ, 278, 499
Berriman, G. 1989, ApJ, 345, 713
Berriman, G., Schmidt, G. D., West, S. C., & Stockman, H. S. 1990, ApJS, 74, 869
Boller, Th., Meurs, E. J. A., Brinkmann, W., Fink, H., Zimmerman, U., & Adorf, H.-M. 1992, A&A, 261, 57
Brandt, W. N., Fabian, A. C., & Pounds, K. A. 1996, MNRAS, 278, 326
Brandt, W. N., Mathur, S., Reynolds, C. S., & Elvis, M. 1997, MNRAS, in press
Brindle, C., Hough, J. H., Bailey, J. A., Axon, D. J., Ward, M. J., Sparks, W. B., & McLean, I. S. 1990a, MNRAS, 244, 577
———. 1990b, MNRAS, 244, 604
Clayton, G. C., & Cardelli, J. A. 1988, AJ, 95, 695
De Grijp, M. H. K., Keel, W. C., Miley, G. K., Goudfrooij, P., & Lub, J. 1992, A&AS, 96, 389
Dickey, J. M., & Lockman, F. J. 1990, ARA&A, 28, 215
Fiore, F., et al. 1997, MNRAS, submitted
Forster, K., et al. 1997, in preparation
Goodrich, R. W. 1989a, ApJ, 340, 190
———. 1989b, ApJ, 342, 224
———. 1995, ApJ, 440, 141
Goodrich, R. W., & Miller, J. S. 1994, ApJ, 434, 82
Grupe, D., Wills, B. J., Wills, D., & Beuermann, K. 1997, A&A, submitted
Heiles, C., Kulkarni, S., & Stark, A. A. 1981, ApJ, 247, L73
Hines, D. C., & Wills, B. J. 1993, ApJ, 415, 82
Lawrence, A., & Elvis, M. 1982, ApJ, 256, 410
Leighly, K. M., Mushotzky, R. F., Yaqoob, T., Kunieda, H., & Edelson, R. 1996, ApJ, 469, 147
Leighly, K. M., et al. 1997, in preparation
Magdziarz, P., & Zdziarski, A. A. 1995, MNRAS, 273, 837
Martel, A. R. 1996, Ph.D. thesis, Univ. California, Santa Cruz
Mathur, S., Elvis, M., & Wilkes, B. 1995, ApJ, 452, 230
Moran, E. C., Halpern, J. P., & Helfand, D. J. 1996, ApJS, 106, 341
Mushotzky, R. F. 1982, ApJ, 256, 92
Nandra, K., George, I. M., Mushotzky, R. F., Turner, T. J., & Yaqoob, T. 1997, ApJ, 476, 70
Netzer, H., & Laor, A. 1993, ApJ, 404, L51
Osterbrock, D. E., & Pogge, R. W. 1985, ApJ, 297, 166
Otani, C. 1996, Ph.D. thesis, Tokyo Univ.
Otani, C., et al. 1996, PASJ, 48, 211
Reynolds, C. S. 1997, MNRAS, 286, 513
Reynolds, C. S., Ward, M. J., Fabian, A. C., & Celotti, A. 1997, MNRAS, in press
Rudy, R. J., Schmidt, G. D., Stockman, H. S., & Moore, R. L. 1983, ApJ, 271, 59
Smith, P. S., Schmidt, G. D., Allen, R. G., & Hines, D. J. 1997, ApJ, 488, 202
Thompson, I. A., & Martin, P. G. 1988, ApJ, 330, 121
Turner, T. J., Netzer, H., & George, I. M. 1996, ApJ, 463, 134
Veilleux, S., & Osterbrock, D. E. 1987, ApJS, 63, 295
Wills, B. J., & Hines, D. C. 1997, in Mass Ejection in AGN, in press
Wills, B. J., Wills, D., Evans, N. J., Natta, A., Thompson, K. L., Breger, M., & Sitko, M. L. 1992, ApJ, 400, 96
Woźniak, P. R., Zdziarski, A. A., Smith, D., Madejski, G. M., & Johnson, W. N. 1997, MNRAS, in press